MULTI-PARAMETER OPTIMIZATION AND EXPERIMENTAL AND NUMERICAL STUDY OF HEAT TRANSFER OF GAS TURBINE BLADE SNUBBER

Mengmeng Liu, Zhiqing Wu, Ju Zhang, Pei-feng Hsu, and C. S. Subramanian
Department of Mechanical and Aerospace Engineering,
Florida Institute of Technology

ABSTRACT

Our earlier work on optimization of the fourth-stage hydrogen gas turbine blade mid-span shroud ring structure (snubber) has been extended in the current work to include more geometrical parameters, i.e., individual fillet radii, to explore more ways of further reducing drag and structural stress. The method involves the problem of optimizing shroud geometry for minimum drag force and maximum component service life (through minimizing the maximum equivalent stress). Fluent and ANSYS Structure software tools were used to simulate the aerodynamics and structural forces and the solution is optimized with the Isight optimization environment. About 4% and ~16% reduction in drag and maximum equivalent stress were achieved, respectively, compared with the original design.

Heat transfer process around the snubber for the fourth-stage hydrogen gas turbine blade is also investigated both experimentally and numerically. The snubber is heated by a thin film heater while air flows around it in the cascade wind tunnel. The thermochromic liquid crystal (TLC) coatings were employed to measure the temperature on the surface of the snubber. The recorded steady state surface temperature distribution is used to calculate the convection heat transfer coefficients. It is observed that the convection heat transfer coefficients are the highest near the leading edge of the snubber. This is also confirmed by numerical simulations.

INTRODUCTION

In gas-powered turbines, the failure modes of the blades include high cycle fatigue, low cycle fatigue, and creep rupture [1]. High cycle fatigue is a situation in which relatively low stresses are applied to the point of interest over long periods of time, resulting in only elastic deformations in the short term; high cycle fatigue generally results in longer fatigue lives than low cycle fatigue, which features greater applied stresses over shorter periods of time, creating plastic deformations in addition to elastic, greatly decreasing the fatigue life of the components [2]. For latter-stage turbine blades, high cycle fatigue is more common, manifesting itself in many forms, but the two forms in which we are most interested are stall flutter and vibration resonance. Stall flutter is described as “an aero-elastic instability wherein, under certain flow conditions, vibratory deflections in the airfoil cause changes in the aerodynamic loading on it that tend to increase, rather than dampen, the deflections” [3]. This flutter is an example of high cycle fatigue that can dramatically shorten the fatigue life of a turbine blade; this problem can be solved by changing the mechanical structure and properties of the blade itself, but to alter a blade’s material properties without damaging the desired aerodynamic properties is a very difficult task [3]. The other failure mode is related to vibration and resonance. There are three ways to lower vibratory stresses including minimizing the applied forces, changing the resonant frequency or increasing the damping of vibration [4]. Thus, the idea of a mechanically-dampening snubber apparatus was developed.

Snubbers, appendages on a turbine blade used to increase the fatigue life of the blades while minimally affecting the flow through the turbine, were initially designed for and applied to steam turbines, but as gas turbine blades increased in length, the need for the implementation of some dampening device between the longer blades of the latter stages of the turbine became clear [3]. A "snubber" is a secondary platform located along the airfoil portion of the blade to damp vibrations caused by twisting, flutter, and flapping of the blade [5]. The desire is that this apparatus will strengthen the turbine blades in order to increase their fatigue lives [3]. However, the implementation of this design innovation is not without drawbacks; the most immediate concern is the alteration of the aerodynamic performance of the turbine [5]. If the addition of the snubber harms the efficiency of the power-producing process itself, then it is not a feasible addition with respect to cost. Additionally, snubbers add additional weight to be borne by the mechanical and structural strength of the turbine blade itself, the design of which may not have been intended to carry such loadings [5]. Thus, the blade rotors and the discs or drums that are used to mount the blade have to be strengthened to account for the increased centrifugal force added by the additional weight of the snubber [6].

In the current work, we are concerned with expanding on the geometric optimization of a snubber geometry for the fourth-stage hydrogen gas turbine blade.

SNUBBER GEOMETRY OPTIMIZATION

The method for solving the problem of optimizing shroud geometry for minimized drag force and maximized component life was derived from our previous work [7, 8]. The essential procedures of the method are rehashed here.

Integrate Numerical Analysis of Fluid Dynamics and Structure

Isight was used to integrate two independently run software, Fluent [9] and Ansys Structure [10], to provide the shroud optimization based on the CFD and FEM results. Integration of the structural and aerodynamic analysis elements under Isight environment allows for significant increase in the rate of design iteration. At the same time Isight allows users to control parameters and examine their effects on one another. This is very useful for the consideration of the two different design aspects. Figure 1 shows the algorithm of obtaining optimized snubber geometry data points. Starting from the top left, Isight will provide a new set of geometry parameters for a new iteration. Using calculator function built in Isight, it translates all parameters into real snubber dimensions. After that, the geometry and fluid-flow control volume will be generated by ANSYS Design modeler and sent to ANSYS Structural/Fluent for structure stress and flow simulations. In the end Isight retrieves all the simulation result and evaluates it for generating the next set of geometry parameters.

Objective Function Definition and Evaluation

After the computational fluid dynamics and structural finite element models of the shroud are integrated in Isight, a method of comparing the results must be developed. The purpose of this objective function is to evaluate the design by considering both the CFD and FEM results.

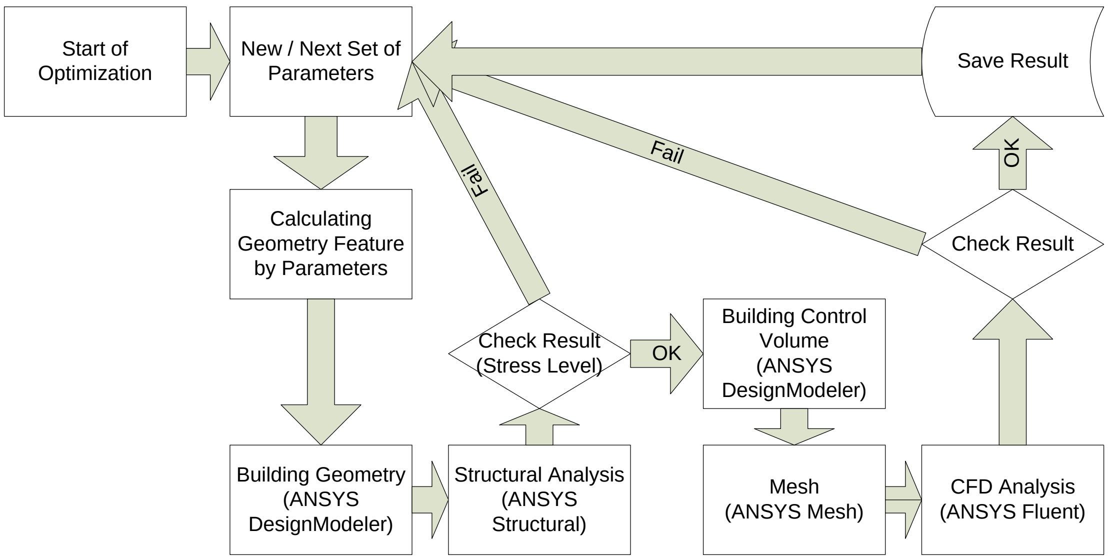

Figure 1. Flow chart of simulation iterations.

The objective of the optimization was to minimize the drag force caused by the snubber while maximizing the fatigue life of the geometry. A comparative approach combining the mean stress against a drag force correlation is used to denote progress with respect to the baseline. According to the Wöhler curve [11], logarithmic fatigue life of blade is proportional logarithmic stress.

$$Obj = \frac{\left(\frac{\sigma}{k}\right)^{1/m} - \left(\frac{\sigma_B}{k}\right)^{1/m}}{\left(\frac{\sigma_B}{k}\right)^{1/m}} - \frac{\overline{vD} - \overline{v_B D_B}}{\overline{v_B D_B}} \approx \frac{\sigma^{1/m} - \sigma_B^{1/m}}{\sigma_B^{1/m}} - \frac{D - D_B}{D_B} \tag{1}$$

In Eq. (1), $(\frac{\sigma}{k})^{1/m}$ is the fatigue life of blade. Constant *k* stands for yielding stress which makes blade life equal to 1, also means instant failure. Constant *m* is slope of Wöhler curve. $\overline{vD}$ is average power loss caused by control volume drag force *D* and flow velocity *v*. Bar denotes the area average over the blade surface control volume. The baseline results for drag and stress are denoted by the subscript “B.” The first term of equation represents the percentage difference of blade fatigue life and the second term represent percentage difference of power loss caused by drag force. Assuming those two numbers are small enough, the equation can be simply summed up. Another assumption is that the average velocity is changing much less than the drag force. This relationship relates the input parameters of the snubber geometry, as well as the desired optimization parameters to arrive at a life-cycle weighted progressive function. The geometric parameters are related by comparing the drag force and the stress results among all data points, and the established baseline starting point’s results. Non-dimensionalization allows conveniently displaying trends of various geometry parameters on the maximum equivalent stress and drag force.

<u>Geometry Modeling</u>

The original geometrical parameters [8] included, as shown in Figure 2, the parameters used in the model are the taper ratio, contact surface width, shape ratio, and pressure and suction side fillet radii.

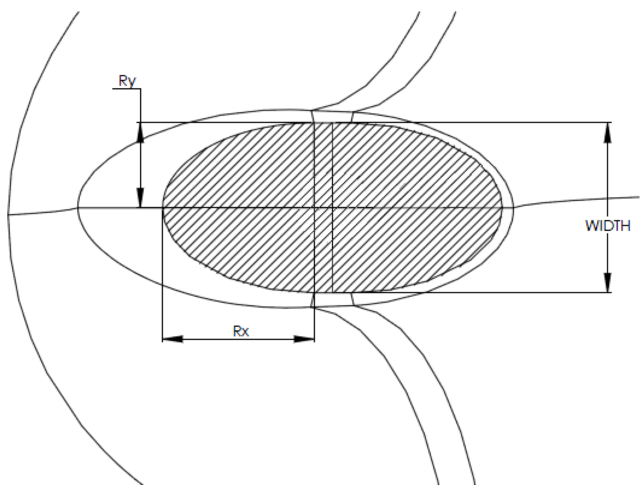

Figure 2. Top view of snubber and definitions of the five-parameter model.

Several options were considered currently for an expanded parameter study, and the decision was made to introduce new parameters in the form of variable fillet radii. This allows for more advanced contours, which means more dynamic control of the geometry is possible. Four parameters for snubber fillet radii were introduced on each side of the blade; Figure 3 below shows the geometrical area of focus and a definition of the variable fillet radii on one side of the blade.

With 8 new radii parameters (4 on each side), a more advanced solution could be pursued to reduce the stress and drag. In order to reduce computational time, the non-fillet radii parameters were held constant from the previous design.

Design of Experiment (DOE) and Latin Hyper Cube

Having refined the analytical models used in the shroud analysis, a method of acquiring data from the design space was desired. Here the design of experiment: Latin hypercube method was utilized. A Latin hypercube explores a multidimensional input parameter design space by generating a collection of results from parameter distribution. This distribution of parametric results was performed automatically through the Isight engine that the numerical models were

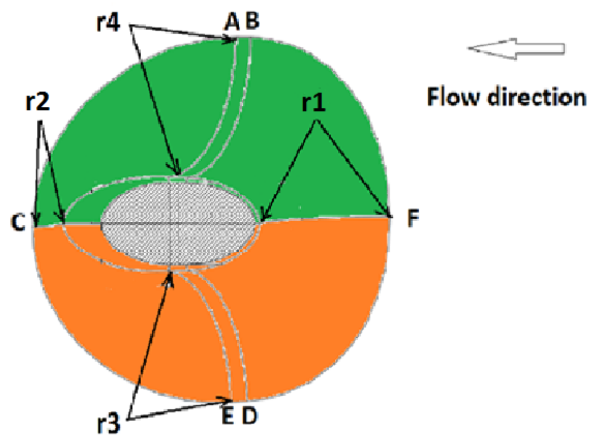

Figure 3. Fillet radii being optimized.

integrated within. Latin hypercube is more useful in a multi-disciplinary optimization of a multi-dimensional design space due to its capability to greatly vary and provide a survey of input parameters over a short period of time.

Current Challenge and Procedure

Due to the complex nature of the geometry, several software issues arose. Most notably, ANSYS Structural had a design limitation whereby the fillet radii were unable to be automatically read in before each iteration. This meant that the radii dimensions have to be set manually before each iteration. This drastically increased the computation time, and required much more effort on the part of the user. With results from the initial five-parameter shroud optimization [8], a starting point for the design was selected. All of the five parameters from previous optimized design were held constant.

EXPERIMENTAL SETUP

For experimentation, a cascading test section to more accurately simulate turbine blade running conditions in the wind tunnel at the FIT has been designed and built. The test section operates between the inlet contraction section and exhaust diffuser of the current wind tunnel and provides the following features to more easily and accurately test the turbine blade/snubber design: a blade section able to hold 5 blade cascade, controllable periodicity, variable angle of attack ($\pm$10 degree rotation of blade section), variable turning angle (30-60 degrees), force/torque measurement capabilities on middle blade, wake survey (Pitot static tube/hotwire anemometer). A picture of the mounted test section is shown in Figure 4. Note that the shape of the blades have a curvature to them, and it is found to be essential to have a test section which followed a similar curvature rather than a straight test section.

In order to examine heat transfer around the snubber in a wind tunnel (rather than the actual gas turbine working condition), heating the snubbers on the center blade in the cascade section was chosen to achieve temperature difference between the snubber surface and freestream. To this end, a thin film heater was wrapped around the pressure side of the snubber and one around the suction side of the snubber. In order to achieve one film heater per side of the blade, two custom designs will be created to fit the geometries of both sides. While adding film heaters to the snubbers, it was tried to make sure not to disturb the geometry of the snubber as this will cause erroneous results. Thermochromic liquid crystal (TLC) coatings were then employed on top of the thin film heaters covering the snubber area to measure the temperature at the surface. Once the steady state surface temperature has been reached, the wind tunnel will be turned on. The air passing over the surface of the snubber will cause a change in the temperature on the surface. The steady state surface temperature will then be recorded and used to calculate the convection heat transfer coefficients.

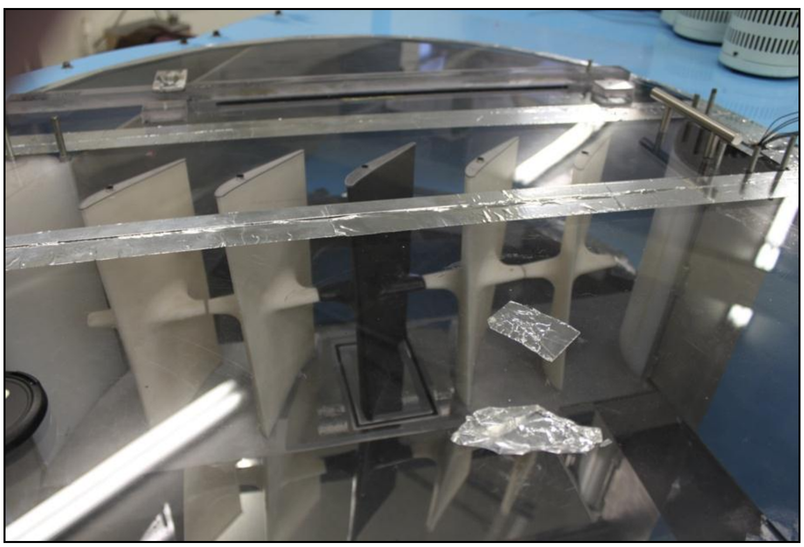

Figure 4. Picture of the cascading test section.

RESULTS

Optimization of Fillet Radii

The previous optimized geometry was based on a five-parameter model. This geometry did not meet the design goal of maximum equivalent stress. New parameters were introduced here to create an even more optimized geometry and hopefully reach the design goals of minimized drag force and maximum equivalent stress. As mentioned earlier, to reduce computation time, the non-fillet radii parameters from previous design were held constant, while 8 new fillet radii parameters (4 per side) were added for optimization.

The comparison of the optimization results is listed in Table 1. The reduction of ~4% and ~16% in drag and maximum equivalent stress were achieved, respectively, compared with the original design. The current optimization result is an improvement over that obtained in [8]. However, it does appear that our 8-radii model has reached its limitations, and the design goal of maximum equivalent stress has yet to be reached. Yet to be explored is the cross section shape. These and other options will be discussed and debated as the optimization process is continued in the future.

	Original Design	[8]	Current
σ	σ_o	14.5%	15.6%
D	D_o	3%	3.9%
Objective function	Obj_o	13%	16.3%

Table 1: Percentage reduction of maximum equivalent stress and drag of current optimization compared to previous designs. Note that the values of original design parameters are proprietary.

Heat Transfer Experiments and Simulation Results

Figure 5a shows the experimental image on the pressure side of the blade for a 16.9 m/s inflow velocity. The experimental image was then processed according to the color- temperature spectrum of the TLC to produce temperature distribution on the snubber surface as shown in Figure 5b. After the temperature distribution was obtained, the convection heat transfer coefficient can be calculated from,

$$h = \frac{Q}{A(T_s - T_\infty)} = \frac{IV}{A(T_s - T_\infty)}$$

where I and V are the current and voltage of the heater, respectively. This is plotted in Figure 6a and is compared with that from a numerical simulation shown in Figure 6b. Note that the uncertainty for the experimental data is found to be approximately 23.5 W/m^2-K. It is observed that, despite all the simplifications made in the numerical simulation, the simulation reproduces the trends of variation in the experimental data reasonably well. In addition, the convection heat transfer coefficients in both vary within approximately the same range and between 180 and 350 W/m$_2$K. The highest values are found near the leading edge in both, the right side edge of the snubber in the image. The average HTC is 395.3 W/m^2-K on suction side, 378.3 W/m^2-K on pressure side. In CFD, the average HTC of the snubber is 315.1 W/m^2-K on suction side, 309.1 W/m^2-K on pressure side.

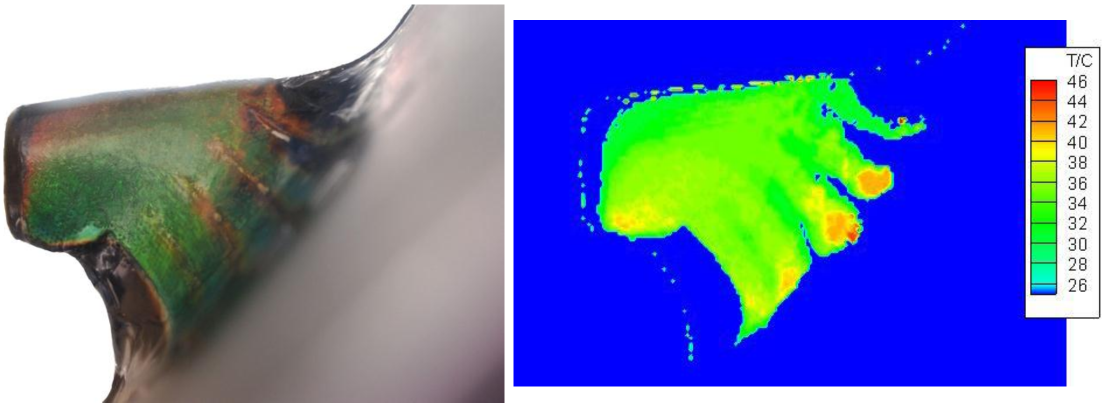

Figure 5. (Left) Experimental thermochromic liquid crystal (TLC) color image during testing with a 16.9 m/s inflow velocity. (Right) Deduced snubber surface temperature (°C) distribution based on the TLC image.

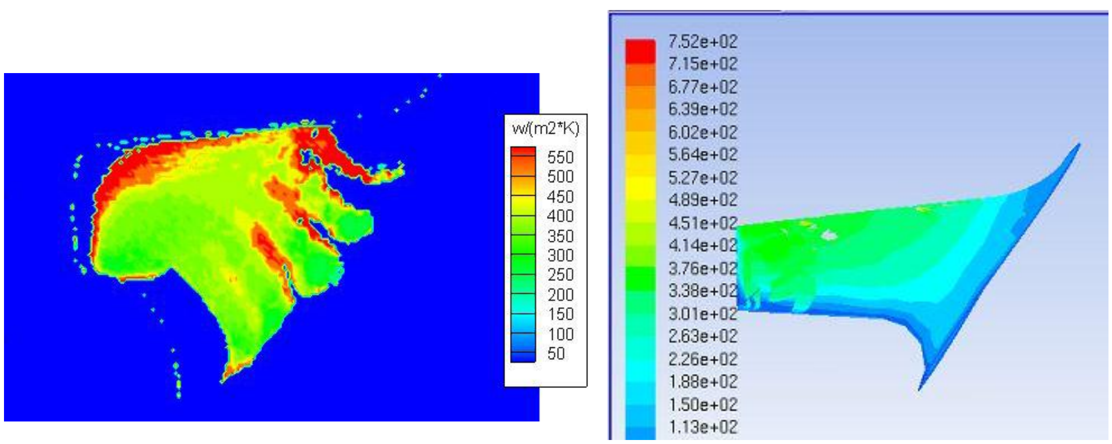

Figure 6. Comparison of convection heat transfer coefficients in experiments (left) and numerical simulations (right).

CONCLUSIONS

Variable-fillet radius on the shroud interface to the blade to allow for more dynamic control and advanced contours was introduced to snubber geometry optimization. Although the targeted maximum allowable stress level to obtain the design life cycle requirement for the shroud was not met in the design optimization process, drag force was indeed reduced by about 1% compared to [8], and 4% compared to the original design (Table 1). In the future, cross section shape or possibly changing the contact surface angle may be explored.

REFERENCES

[1] Naeem, Mehdi Tofigi, Seyed Ali Jazareyi, and Nesa Rezamahdi, 2008, “Failure Analysis of Gas Turbine Blades.” IAJC-IJME International Conference.

[2] Callister, Jr., William D. Materials Science and Engineering: An Introduction. Seventh Edition.

Wiley: New York, 2007.

[3] Pfeifer, Nathan R., John P. Thomas, and Wally N. Dangerfield. "Aerodynamically optimized mid-span snubber for combustion turbine blade." PatentStorm. 9 Dec. 1997.

[4] Narishma, S., G. Venkata Rao, and S. Ramakrishna. "Stress and Vibration Analysis of a Gas Turbine Blade with a Cottage-Roof Friction Damper Using Finite Element Method." National Conference on Machines and Mechanisms. 17 Dec. 2009.

[5] Huebner, Norbert. "Blade with optimized vibration behavior." PatentStorm. 7 Jan. 2003.

[6] Fuller, John R. D. "Vibration damped rotor blades for turbomachines." PatentStorm. 17 Jul. 1984.

[7] Wu, Y., Funk, C. K., Hsu, P., Le Moine, J., Zhou, R., Subramanian, C. S., Campell, C. X., and Marra, J. J., "Design Optimization of Turbo-Machinery Components with Independent FEA and CFD Tools in an Optimization Software Environment - a Mid-Span Shroud Ring Study Case," in proceedings of ASME IMECE 2011.

[8] Wu, Y., Le Moine, J., Hsu, P., Funk, C. K., Subramanian, C. S., Campell, C. X., S. R. Miller and Marra, J. J., "Multi-disciplinary Optimization of Mid-Span Shround Ring Structure: A Multi-parameter Geometry Study case," in proceedings of ASME Turbo Expo 2012.

[9] ANSYS,Inc., ANSYS FLUENT 12.0 User's Guide, April, 2009(ANSYS,Inc.).

[10] ANSYS, Inc., ANSYS Workbench Scripting Guide, 2009, ANSYS, Inc.

[11] D. Coutsouradis, 1994, "Materials for advanced power engineering," Volume 2, Springer.